VOL. 13, NO. 6, JUNE 2018 ISSN 1990-6145
ARPN Journal of Agricultural and Biological Science

www.arpnjournals.com

NUMERICAL MODEL ESTIMATION OF BIOMETHANE PRODUCTION USING AN ANAEROBIC CSTR: MODEL FORMULATION, PARAMETER ESTIMATION AND UNCERTAINTY/SENSITIVITY ANALYSIS

Hatem Yazidi[1], Geraint Bevan[2], Joseph V Thanikal[1], Ole Pahl[2] and Colin Hunter[2]
[1]Waste to Energy Laboratory, Caledonian College of Engineering, Seeb, Sultanate of Oman
[2]School of Engineering and Built Environment, Glasgow Caledonian University, Cowcaddens Rd, Glasgow G4 0BA, United Kingdom
E-Mail: hatem@caledonian.edu.om

ABSTRACT

In this paper, an innovative complex numerical model is proposed for simulating the anaerobic biogas production potential of organic waste materials both for full-scale anaerobic plant design and operation decisions and for laboratory and pilot scale co-digestion research. The model facilitates, in particular, the understanding of co-digestion and mixture effects by application of uncertainty and global sensitivity analysis. This allows multi-dimensional parameter analysis so that uncertainties and the main sensitivities can be identified among the model parameters, with a special focus on those leading to digester failure. The initial application of the complex model to ongoing lab-scale anaerobic co-digestion processes revealed that the hydrolysis and acidogenesis phases are the most affecting steps of the methane production. In particular, the following parameters have been found to contribute the most to the variance of the complex model's estimate of methane production: polymer hydrolysis rate; specific acidogens maximum growth rate; saturation constant for acidogens, the specific acetoclastic methanogens maximum growth rate; saturation constant for acetoclastic methanogens; and the gas-liquid mass transfer coefficient for methane.

Keywords: anaerobic co-digestion, statistical sampling, uncertainty analysis, global sensitivity analysis.

1. INTRODUCTION

The main anaerobic co-Digestion process (AcoD) outputs are the production of biogas. This mechanism can be seen as a clean and sustainable process for producing electricity through biogas combustion. The AcoD process is orchestrated by a consortium of microorganisms that degrade organic substrates present in the biological wastes. AcoD can, also, have a key role in mitigating the adverse effect of uncontrolled dumping all types of solid waste by transforming the organic fraction of it into fertilizer [1], [2]. Nevertheless, from the practical point of view, there are few problems arising from the industrialization of AcoD process which needs to be further investigated. They generally are the same as those encountered in any processing industry, mainly controlling the biotechnological mechanisms of an AcoD plant to avoid any product failure that evolves delays in the final delivery. In Generally, AcoD plant designers and operators actually seek for optimization of the degree of the initial substrates with inoculum mixing to lower the cost and also the environmental impact without compromising the biogas output [3]. The solution depends closely on and can be subject to the substrate type as well as to the process flow dynamics in the AcoD plant digesters. The latter is in turn determined by the physical parameters of the digestion vessels, inflow mode, sludge rheology and, crucially mixing systems. In addition, limiting steps to AcoD can also be considered fatal to the system performance. This include the acetogenesis mechanism [4]-[6], methanogenesis mechanism [7], hydrolysis mechanism [8] and disintegration mechanism [9], [10].

This paper introduces a useful numerical tool that reduces considerably the uncertainty about AcoD mechanisms: a complex deterministic dynamic mathematical model, adapting the operational conditions to simulate the co-digestion processes that can indicate the best settings to maximize the performance of the AcoD process.

The rest of the paper is organized as follows; Section (2) introduces the experimental setup including both the substrates and inoculum preparation, the reactor design and gives an insight on the experimental data set used in this work. Then, Section (3) presents the dynamic numerical model structure and assumptions. Section (4) details the process followed to calculate the model best parameters values. Section (5) details the approach used in this paper to define which one of the model parameters influence the most the model outputs. This can be done by verifying the model parameters uncertainty using the Uncertainty Analysis (UA) method. Also, we proposes in the same section to evaluate the model outputs variations due to different input sources. This is done by applying the Sensitivity Analysis (SA) method. We present our results and discuss them in Section (6). We conclude, in Section (7), by discussing the perspectives and the limitations of our approach.

2. MATERIAL AND METHODS

2.1 Substrates preparation

The fruit and vegetable waste were used in this study and were collected from Al Mawalah Central Market in Muscat (The Sultanate of Oman). The fatty oil was collected from nearby restaurants. All solid substrates were shredded into small pieces and stored at 4 degrees Celsius and characterised for total solids (TS), Suspended solids (SS) and Volatile suspended solids (VS) as detailed in Table-1. The substrates were characterised as per

APHA (2012) methods [11]. The cooked oil contains rich amounts of lipids. At higher concentration lipids are considered to be problematic components for better performance of an AcoD process [12]. Fatty oil is often co-digested with other substrate types to reduce the lipid concentration in the digester [13]. Consequently, problems such clogging, adsorption to biomass (affecting the mass transfer process), microbial inhibition due to the degradation could be a trigger for enhancing the long-chain fatty acids (LCFA). An imminent by-product of the lipids transformation which increase the digetsers acidification process and, therefore, increase the chances to bioreactor collapsing.

Table-1. Characteristics of substrates.

Param.	Po.	Car.	Spin.	On.	Tom.	Lett.	App.	Org.	Grp.	POM	WatM
PH	4.5	4.8	5.6	7.82	7.78	7.70	5.74	3.89	3.42	5.31	6.79
COD ($g \cdot Kg^{-1}$)	220	180	90	52	310	145	120	60	80	210	150
MC (%)	99.36	89.69	99.7	85.56	99.5	88.54	90.47	95.92	98.8	72.63	95.35
TS ($g \cdot g^{-1}$)	0.34	0.17	0.13	0.25	0.09	0.11	0.21	0.25	0.36	0.38	0.14
VS ($g \cdot g^{-1}$)	0.16	0.07	0.05	0.12	0.04	0.05	0.12	0.12	0.16	0.20	0.08
SS ($g \cdot g^{-1}$)	0.18	0.09	0.08	0.13	0.05	0.06	0.13	0.14	0.20	0.25	0.09

Po: Potatoes, Car: Carrots, Spin: Spinach, On: Onion, Tom: Tomatoes, App: Apples, Org: Oranges, Grp: Grapes, POM: Pomegranate, WAT: Watermelon.
MC: Moisture Content, TS: Total Solids, VS: Volatile Solids and SS: Suspended Solids.

2.2 Reactor design and operation

A multi-series of experiments were performed in an identical two double-walled bio-reactors of 6 liters effective volume (BR) maintained at 38°C by a regulated water bath (Figure 1). Mixing in the BRs was done by a system of magnetic stirring. The pH inside the reactor was continuously monitored online using Metler Toledo pH probe Inpro 4260i and maintained at 7.5±0.5.

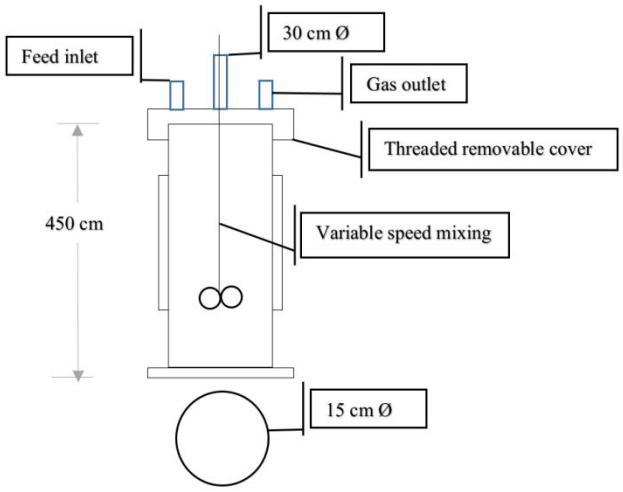

Figure-1. Schematic diagram of the laboratory-scale digester.

The BR was operated in batch mode without withdrawal (semi-continuous). The flow rate was determined by each batch assay. The batch end was considered once the flow rate reached a threshold value of 1 ml h^{-1}. The reactor was fed with vegetable substrates at an OLR varying from 1.0 to 6.0 g [VS] $d^{-1} l^{-1}$, respectively.

2.3 Inoculum preparation

A quantity of 700 g of Granular sludge obtained from an Up-Flow Anaerobic Sludge Blanket fixed-Bed (UASB) reactor treating sugar factory effluent was used to inoculate our 6l volume bioreactor. In addition, we fed our BR with ethanol during the start-up phase of our experiments to observe the biological activity of the inoculum.

2.4 The experimental data

The total of 120 days of cumulative biogas production temporal series plot is shown in Figure 2, where the biogas production is observed to be exponential to the increase in Organic Loading Rate (OLR). Nevertheless, the reactor experienced the problem of mixing when higher quantities of solids are added to the reactor.

It is worth noting that some failures such leaks, tube clogging and so forth have slightly perturbed the initial protocol.

Figure-3 displays some of the batches conducted for fruits co-digestion. It shows that the increase in the organic load conditions from1 to 5 g [VS] $d^{-1} l^{-1}$ corresponds to an increase of cumulative biogas. This was observed during the AcoD batch tests performed under mesophilic conditions for mixing of fruits along with Granular sludge obtained from an Up-Flow Anaerobic Sludge Blanket Anaerobic fixed-Bed.

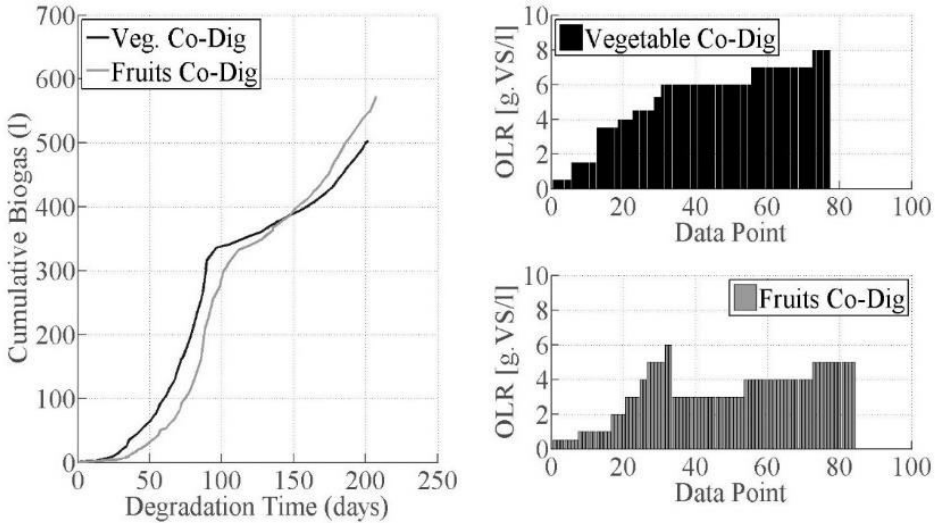

Figure-2. Cumulative biogas production (left plot) vs. organic loading rate for fruit, vegetables and cooked oil waste (right plots).

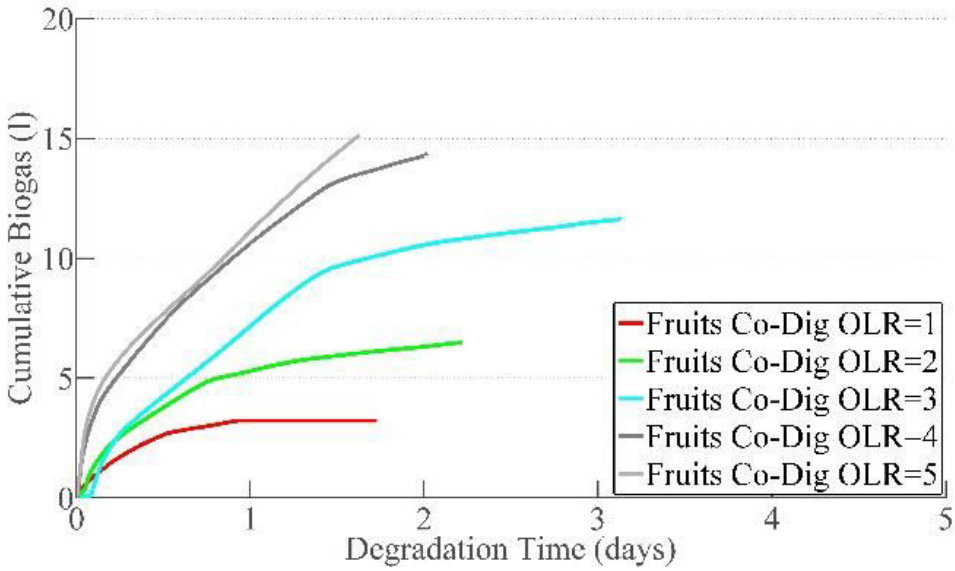

Figure-3. Fruits co-digestion cumulative biogas production tests.

3. Model assumption and description

3.1 Model assumptions

The selection process of any dynamic model shall be based on the trade-off between the model complexity, flexibility and avidity (determined by the number of state variables and parameters included). In this paper, we present a model that is data-driven and mechanistically describing digestion dynamic processes. The selected model is partially driven by the amount of a priori knowledge available on the system: a combination of multiple parameters such as measured data, bioreactor design, yields coefficients, bacterial growth rates, substrates initial concentrations and error estimation.

Although mathematical models are efficient tools used to optimize an AcoD process, it is worth considering that obtaining reliable parameters of an anaerobic digestion is very challenging. In fact, the AcoD processes compass a very wide range of microorganisms and compounds. Nevertheless, in this work we assume that the bacterial populations can be divided into five main groups of homogeneous characteristics and that the proposed model can be described by six-stage processes as described in the next Section here below. In addition, we assume that the reactor behaves like a perfectly mixed tank and that the biomass is uniformly distributed inside the fermentor.

3.2 Model description

The reactions and processes occurring in the anaerobic digestion proposed system to model are simplified into the following general steps (Figure-4). The

model equations are displayed in Appendix A. As shown in Figure-4, the proposed model structure is typically composed of the combination of hydrodynamics terms, liquid−gas terms, and conversion (kinetic + yields) terms. The conversion and liquid-gas transfer terms contain all the parameters to be calibrated, while the terms related to the hydrodynamics are ideally characterized by the known values of the influent. At the first step, the polymeric substrate (S_0) is hydrolyzed using enzymes, producing fermentable monomers (S_1). Then, at the second step, the fermentable monomers (S_1) are transformed into Propionic acid (S_2), soluble hydrogen (S_3), soluble carbon dioxide (S_4), Acetic acid (S_5) and Butyric acid (S_6) by acidogenic bacteria (X_1). The third step is characterized by the Propionic acid (S_2) transformation into H_2 (S_3), followed by its transformation into CO_2 (S_4) and Acetic acid (S_5) by syntrophic bacteria type A (X_2). The fourth step is the transformation of the Acetic acid (S_5) into methane (S_7) and CO_2 (S_4) by Acetoclasticmethanogenic bacteria (X_4). The fifth step correspond to the transformation of the Butyric acid (S_6) into H2 (S_3) and acetic acid (S_5) by syntrophic bacteria B (X_5). In the sixth step, both CO_2 and H_2 are used by the hydrogenotrophic-methanogenic bacteria (X3) to generate methane (S_7), and transfer of CO_2, H_2 and methane between the gas and liquid phases of the bioreactor.

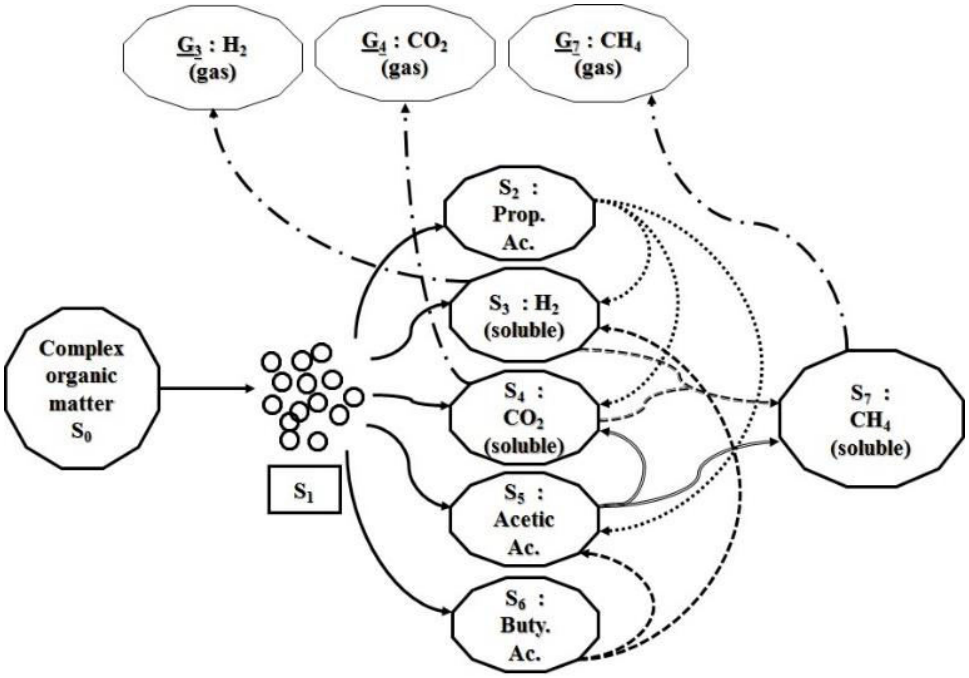

Figure-4. Diagram of main reactions and biochemical processes undertaken by the proposed model.

4. Model parameter optimization procedure

The model developed in the previous sections includes seventy-eight parameters that have to be identified from experimental data. This step is highly important to assure a wide range of validity of our model but also very difficult to model. For more practicability a structural identification problems, we have chosen an approach based on two points. We first decoupled the model parameters to be estimated into three groups: the kinetic parameters (K_h, μ_{MAX1}, K_{S1}, μ_{MAX2}, K_{S2}, μ_{MAX3}, K_{S3}, μ_{MAX4}, K_{S4}, μ_{MAX5}, K_{S5}, K_{S6}) the transfer coefficient (K_{la3}, K_{la4}, K_{la7}) and the yield coefficients. Our main motivation behind this decoupling lies in the high difficulty of kinetics modelling in general lead to a large uncertainty in bioprocess dynamical models. Secondly, we applied an optimisation algorithm to construct optimisation problems in MATLAB and solve them.

The mathematical description of the optimization algorithm approach is as follows:

- **Step 1:** Applying an estimator of the parameter θ that minimizes the sum of the squares of the error represented by the following cost function:

$$J \cong \frac{1}{2}\sum_{i=1}^{N} \epsilon_i^2 = \frac{1}{2}(z - H(\theta))^T (z - H(\theta)) \quad (1)$$

- **Step 2:** Minimization of J w.r.t θ yields:

$$\frac{\partial J}{\partial \theta} = -2\left(z - H(\hat{\theta})\right)^T \frac{\partial H(\hat{\theta})}{\partial \theta} = 0$$

where $\hat{\theta}$ is the parameter value that minimizes the cost function.

5. Model uncertainty and sensitivity analysis

Determining the strength of the relation between a given uncertain input and the output is the job of

sensitivity analysis. Hence, we applied the US technique in this manuscript.

5.1 Uncertainty analysis (UA)

It is essential to verify the possible effects of the error that different parameters can possibly impart on the model outputs. One approach is to perturb each parameter in order to create a spectrum of possible parameter values. This can be made by using Monte-Carlo (MC) methods which are one of the most robust techniques used to generate numerical random set of data from a given probability distribution. This can be done through the implementation a sampling process called Latin hypercube sampling technique (LHS). The probability distributions of the model parameters are the source from which the random data were sampled. Each combination of the dynamic model inputs is evaluated and the results can be used to both determine the uncertainty in model output and perform sensitivity analysis. It is suggested to start by generating a large number of samples to have higher chances in having the most representative input factor distributions through sampling which reduces under-sampling to zero. To address this problem the Latin hypercube sampling algorithm was specifically adopted [14].

The LHS technique has two benefits, (1) allows an estimation of the dynamic model outputs and, (2) involves only fewer samples than the classic random sampling to determine the same accuracy [15]. The steps needed to apply LHS are as follows:

a) **Step 1:** each parameter distributions were divided into N equal probability intervals which were then sampled. The sampling size N shall be at least p+1, where p is the number of parameters;

b) **Step 2:** each interval was sampled once (without replacement) by randomly selecting values;

c) An LHS matrix is generated which as N rows of the number of simulations (sample size) and of p columns corresponding to the number of varied parameters.

d) Each combination of p parameters with N perturbations is injected into the model and provides the respective solution.

5.2 Sensitivity analysis (SA)

The application of sensitivity analysis will help determining the model critical parameters that control the model output. Global SA is an innovative approach for determining which reactions and processes contribute most to the behaviour of the overall system.

We began by visualizing the scatter plot to investigate the linearity between model inputs and outputs. We also calculated the Pearson correlation coefficient (CC) and the partial rank correlation coefficient (PRCC). For nonlinear non-monotonic trends, we deployed methods based on the decomposition of model output variance. Among the foremost methods based on the variance decomposition, we used in this work the one called Sobol method. We also included to our analysis the calculation of the extended Fourier amplitude sensitivity test (eFAST) [17, 18]. However, it is important to mention here that we used both PRCC and eFAST to measure two different model properties which are: (1) PRCC provided us information about the monotonicity characterizing the relationships between a given parameter and the model outputs after the linear effects on the model outputs of the remaining parameters were discounted, and (2) eFAST provided us information of the variance fraction accounted for by individual parameters and groups of parameters. However, we chose here the best-case scenario which is using both of the two indexes.

6. DISCUSSIONS

The PRCC indexes provided us with answers concerning the variability of our dynamic model outputs in response to the increase (or decrease) of a specific parameter. Thus, the usage of PRCC revealed useful information on which parameters to target if we want to achieve specific goals (e.g., control or regulation of the biogas production). Furthermore, we were able to significantly define the set of parameters that can be used to determine how to efficiently decrease Volatile Fatty Acids (VFA) load or increase methane responses (by both timing and magnitude). On the other hand, eFAST as a variance-based method helped us to quantify the impact of the parameter uncertainty which may have the greatest influence on output variability. Our results confirmed that our deterministic model simulation, after applying the parameter estimation algorithm, was able to fit well with the observations (Figure-5).

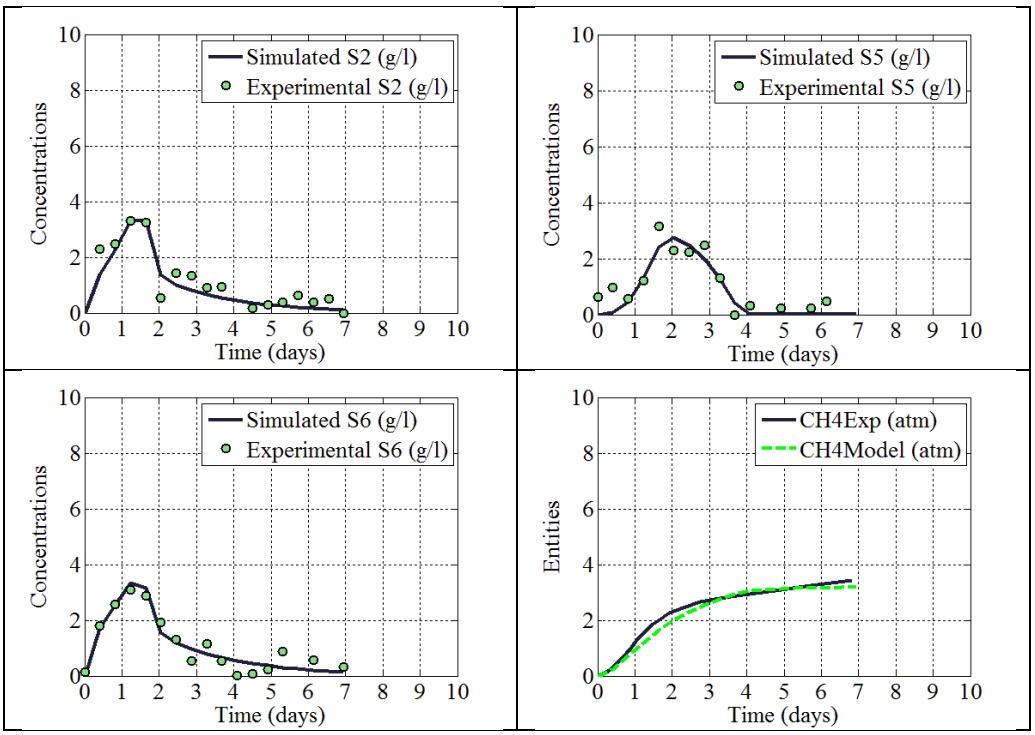

Figure-5. Complex dynamic model variables comparison versus experiments. S2: Propionic acid, S5: Acetic acid and S6: Butyric acid.

After, we applied the LHS scheme with the sample size N taken equal to 1500. Each parameter was independently sampled from normal probability density function. For each sample (parameter combination), we run the model. The time-point chosen to perform both the sensitivity and the uncertainty analysis was taken to be equal to the end of the duration of our experiments which is corresponding to the final methane production.

Our UA demonstrated that PRCC provided nine significant ($p<0.01$) identified most influenced parameters on the model outputs (methane): K_h, μ_{MAX1}, K_{S1}, μ_{MAX3}, K_{S3}, K_{S4}, K_{S5}, K_{S6} and K_{la7} (Figure-6). The positive sign of the PRCC indexes corresponding to the Polymer hydrolysis rate, Maximum acidogens growth rate and Gas-liquid mass transfer coefficient for CH_4, demonstrates that in the case we increase those parameters, the methane production increases. On the other hand, the negative sign of the PRCC indexes relative to the Saturation constant for acidogens and the saturation constant for acetoclastic methanogens, indicates that in the case we increase those parameters, the methane production decrease.

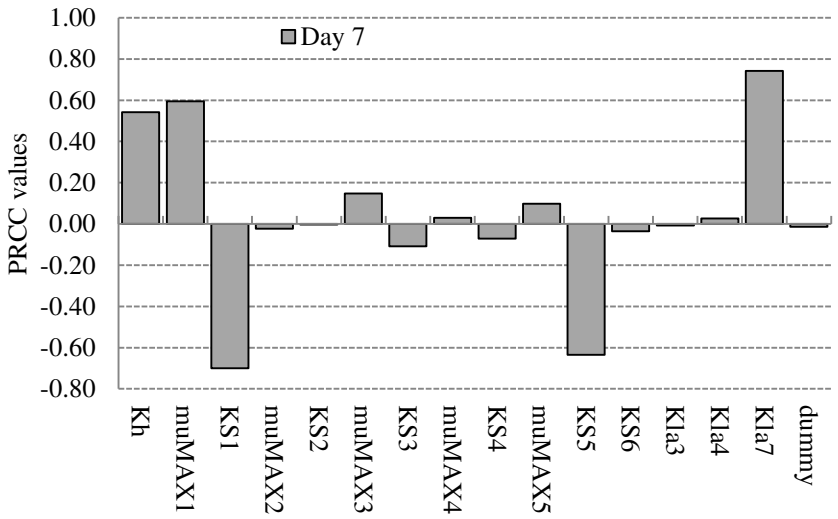

Figure-6. PRCC performed on the AcoD complex model. The reference output is the methane gas production at t = 7 days (end of experiment). PRCC results are calculated using a sample size N=1500.

First order Si and total order Sticorresponding to each parameter are shown in Figure-7, including a dummy parameter [16]. This was used as a screening method.

The calculation of eFAST indexes demonstrated that the sets of significant parameters returned are mostly the same displayed by the PRCC indexes results and are generally have smaller. However, in the case where the same parameter is calculated, the rank is different between two approaches. For example, the values the maximum acetoclastic methanogens (μ_{MAX4}) was found to be clearly detected by eFAST approach. This make sense because the anaerobic methane production is a process very sensitive to acetate since they form about 70% of the methanogenic substrates in anaerobic digestors and is the only dicarbon substrate that methanogenic bacteria can degrade completely.

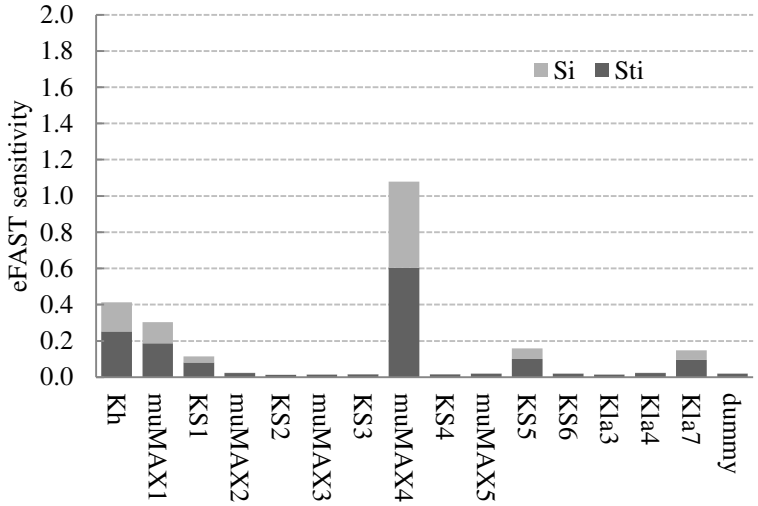

Figure-7. eFAST results with resampling and significance testing. Search curves were resampled five times (NR = 5), for a total of 1285 model evaluations.

7. CONCLUSIONS

In conclusion, a complex AcoD model was proposed to simulate anaerobic co-digestion processes evolved in an anaerobic CSTR. Our results showed a good concordance between partial rank correlation coefficient (PRCC) and the extended Fourier amplitude sensitivity test (eFAST). The parameters that influenced the most the methane production (model output CH_4) were K_h, μ_{MAX1}, K_{S1}, μ_{MAX4}, K_{S5} and K_{la7}.

We found that the increase of the polymer hydrolysis rate (Kh) was effective on the increase of the final methane production. In addition, eFAST, indicated that (Kh) uncertainty index has the second greatest impact on the methane variability. We were able to identify the parameters (i.e. biological mechanisms) that control our model methane estimation. This would allow distinguishing the importance of using of mathematical models to simulate the AcoD systems.

ACKNOWLEDGMENT

The laboratory experimental material used in this research work was a part of the funded research (Grant 63) from the "The Research Council of Oman" (TRC), The Sultanate of Oman.

REFERENCES

[1] H. Bouallagui, R. Ben Cheikh, L. Marouani and M. Hamdi. 2003. Bouallagui_2003_Mesophilic biogas production from fruit and vegetable waste in a tubular digester. 86: 85-89.

[2] H. Yazidi and J. V. Thanikal. 2016. Nonlinear kinetic modelling of anaerobic biodegradation of fruit and vegetable waste together with cooked oil. Int. J. Adv. Res. Biol. Sci. 3(5): 109-121.

[3] D. Dochain. 2013. Automatic control of bioprocess. 53(9). John Wiley & Sons, Inc., ISTE Ltd.

[4] D. J. Hills and D. W. Roberts. 1981. Anaerobic digestion of dairy manure and field crop residues. Agric. Wastes. 3(3): 179-189.

[5] J. D. Bryers. 1985. Structured modelling of the anaerobic digestion of biomass particles. Biotechnol. Bioeng. 27: 638-649.

[6] H. Siegrist, D. Renggli and W. Gujer. 1993. Mathematical modelling of anaerobic mesophilic sewage sludge treatment. In Water Science and Technology. 27(2): 25-36.

[7] R. Moletta, D. Verrjer and G. Albagnac. 1986. Dynamic modelling of anaerobic digestion. Water research. 20(4): 427-434.

[8] V. A. Vavilin, S. V. Rytov, L. Y. Lokshina, J. A. Rintala and G. Lyberatos. 2001. Simplified hydrolysis models for the optimal design of two-stage anaerobic digestion. Water Res. 35(17): 4247-4251.

[9] D. J. Batstone *et al*. 2002. The IWA Anaerobic Digestion Model No 1 (ADM1). Water Sci. Technol. 45(10): 65-73.

[10] D. J. Batstone, J. Keller and J. P. Steyer. 2006. A review of ADM1 extensions, applications, and analysis: 2002-2005. Water Science and Technology. 54(4): 1-10.

[11] APHA. 2012. Standard Methods for the Examination of Water and Wastewater. Stand. Methods. p. 541.

[12] L. Appels *et al.* 2011. Anaerobic digestion in global bio-energy production: Potential and research challenges. Renew. Sustain. Energy Rev. 15(9): 4295-4301.

[13] H. Yazidi and J. V. Thanikal. 2015. Biodegradability and Bio Methane Potential of Vegetable, Fruit and Oil Fraction in Anaerobic Co. Int. J. Curr. Res. 7(7): 18379-18382.

[14] J. C. Helton, F. J. Davis and J. D. Johnson. 2005. A comparison of uncertainty and sensitivity analysis results obtained with random and Latin hypercube sampling. Reliab. Eng. Syst. Saf. 89(3): 305-330.

[15] M. D. Mckay, R. J. Beckman and W. J. Conover. 2000. A Comparison of Three Methods for Selecting Values of Input Variables in the Analysis of Output from a Computer Code. Technometrics. 42(1): 55.

[16] A. Saltelli, M. Ratto, S. Tarantola and F. Campolongo. 2006. Sensitivity analysis practice: A guide to scientific models. 91(10-11).

[17] S. Marino, I. B. Hogue, C. J. Ray and D. E. Kirschner. 2008. A methodology for performing global uncertainty and sensitivity analysis in systems biology. J. Theor. Biol. 254(1): 178-196.

[18] A. Saltelli. 2002. Making best use of model evaluations to compute sensitivity indices. Comput. Phys. Commun. 145(2): 280-297.

Appendix A

The dynamic model set of ordinary differential equations:

$$\frac{dS_0}{dt} = \frac{Q}{V}\left(S_{0_{in}} - S_0(t)\right) - r_h$$

whereby $r_h(t) = k_h \cdot S_0(t)$

$$\frac{dS_1}{dt} = \frac{Q}{V}\left(S_{1_{in}} - S_1(t)\right) + Y_{S0S1} \cdot r_h(t) - Y_{S1X1} \cdot r_{S_1X_1}(t) - Y_{S1S2} \cdot r_{S_2X_1}(t) - Y_{S1S3} \cdot r_{S_3X_1}(t) - Y_{S1S4} \cdot r_{S_4X_1}(t) - Y_{S1S5} \cdot r_{S_5X_1}(t) - Y_{S1S6} \cdot r_{S_6X_1}(t)$$

$$\frac{dX_1}{dt} = \frac{Q}{V}\left(X_{1_{in}} - X_1(t)\right) + r_{S_1X_1}(t)$$

$$\frac{dS_2}{dt} = \frac{Q}{V}\left(S_{2_{in}} - S_2(t)\right) + r_{S_2X_1}(t) - Y_{S2X2} \cdot r_{S_2X_2}(t) - Y_{S2S3} \cdot r_{S_3X_2}(t) - Y_{S2S4} \cdot r_{S_4X_2}(t) - Y_{S2S5} \cdot r_{S_5X_2}(t)$$

$$\frac{dX_2}{dt} = \frac{Q}{V}\left(X_{2_{in}} - X_2(t)\right) + r_{S_2X_2}(t)$$

$$\frac{dS_3}{dt} = \frac{Q}{V}\left(S_{3_{in}} - S_3(t)\right) + r_{S3X1}(t) + r_{S3X2}(t) + r_{S3X5}(t) - Y_{S3X3} \cdot r_{S3X3}(t) - Y_{S3S7} \cdot r_{S7X3}(t) - Kla_3 \cdot (S_3(t) - S_3^*(t))$$

whereby $S_3^*(t) = H_3 \cdot G_3(t)$

$$\frac{dX_3}{dt} = \frac{Q}{V}\left(X_{3_{in}} - X_3(t)\right) + r_{S3X3}(t)$$

$$\frac{dS_4}{dt} = \frac{Q}{V}\left(S_{4_{in}} - S_4(t)\right) + r_{S4X1}(t) + r_{S4X4}^*(t) + r_{S4X2}(t) - Y_{S4X3} \cdot r_{S3X3}(t) - Y_{S4S7} \cdot r_{S7X3}(t) - Kla_4 \cdot (S_4(t) - S_4^*(t))$$

whereby $r_{S4X4}^*(t) = Y_{S4X4} \cdot r_{S4X4}(t)$ and $S_4^*(t) = H_4 \cdot G_4(t)$

$$\frac{dS_5}{dt} = \frac{Q}{V}\left(S_{5_{in}} - S_5(t)\right) + r_{S5X1}(t) + r_{S5X5}^*(t) + r_{S5X2}(t) - Y_{S5X4} \cdot r_{S4X4}(t) \cdot r_{S4X4}^*(t) - Y_{S5S7} \cdot r_{S7X4}(t)$$

whereby $r_{S5X5}^*(t) = Y_{S5X5} \cdot r_{S5X5}(t)$

$$\frac{dX_4}{dt} = \frac{Q}{V}\left(X_{4_{in}} - X_4(t)\right) + r_{S4X4}(t)$$

$$\frac{dS_6}{dt} = \frac{Q}{V}\left(S_{6_{in}} - S_6(t)\right) + r_{S6X1}(t) - Y_{S6X5} \cdot r_{S5X5}(t) - Y_{S6S5} \cdot r_{S5X5}^*(t) - Y_{S6S3} \cdot r_{S3X5}^*(t)$$

whereby $r_{S3X5}^*(t) = Y_{S3X5} \cdot r_{S5X5}(t)$

$$\frac{dX_5}{dt} = \frac{Q}{V}\left(X_{5_{in}} - X_5(t)\right) + r_{S5X5}(t)$$

$$\frac{dS_7}{dt} = \frac{Q}{V}\left(S_{7_{in}} - S_7(t)\right) + r_{S7X3}(t) + r_{S7X4}(t) - Kla_7 \cdot (S_7(t) - S_7^*(t))$$

whereby $S_7^*(t) = H_7 \cdot G_7(t)$

$$\frac{dG_3}{dt} = \frac{RT}{V_g} \cdot \left[\left[Kla_3 \cdot (S_3(t) - S_3^*(t)) \cdot \frac{V}{M_{H_2}}\right] - \dot{M} \cdot V \cdot \frac{G_3(t)}{P_T}\right]$$

$$\frac{dG_4}{dt} = \frac{RT}{V_g} \cdot \left[\left[Kla_4 \cdot (S_4(t) - S_4^*(t)) \cdot \frac{V}{M_{CO_2}}\right] - \dot{M} \cdot V \cdot \frac{G_4(t)}{P_T}\right]$$

$$\frac{dG_7}{dt} = \frac{RT}{V_g} \cdot \left[\left[Kla_7 \cdot (S_7(t) - S_7^*(t)) \cdot \frac{V}{M_{CH_4}}\right] - \dot{M} \cdot V \cdot \frac{G_7(t)}{P_T}\right]$$

Table-A1. Model's reaction rates.

	$r_{S_iX_j}$: *i from* 1 *to* 7 *and j from* 1 *to* 5				
	X_1	X_2	X_3	X_4	X_5
S_1	$\mu_1 \cdot X_1$				
S_2	$Y_{S2X1} \cdot \mu_1 \cdot X_1$	$\mu_2 \cdot X_2$			
S_3	$Y_{S3X1} \cdot \mu_1 \cdot X_1$	$Y_{S3X2} \cdot \mu_2 \cdot X_2$	$\mu_3 \cdot X_3$		$Y_{S3X5} \cdot \mu_5 \cdot X_5$
S_4	$Y_{S4X1} \cdot \mu_1 \cdot X_1$	$Y_{S4X2} \cdot \mu_2 \cdot X_2$		$\mu_4 \cdot X_4$	
S_5	$Y_{S5X1} \cdot \mu_1 \cdot X_1$	$Y_{S5X2} \cdot \mu_2 \cdot X_2$			$\mu_2 \cdot X_5$
S_6	$Y_{S6X1} \cdot \mu_1 \cdot X_1$				
S_7			$Y_{S7X3} \cdot \mu_3 \cdot X_3$	$Y_{S7X4} \cdot \mu_4 \cdot X_4$	

where:

$$\mu_1 = \mu_{MAX1} \cdot \frac{S_1}{K_{S_1} + S_1}$$

$$\mu_2 = \mu_{MAX2} \cdot \frac{S_2}{K_{S_2} + S_2}$$

$$\mu_3 = \mu_{MAX3} \cdot \frac{S_3}{K_{S_3} + S_3} \cdot \frac{S_4}{K_{S_4} + S_4}$$

$$\mu_4 = \mu_{MAX4} \cdot \frac{S_5}{K_{S_5} + S_5}$$

$$\mu_5 = \mu_{MAX5} \cdot \frac{S_6}{K_{S_6} + S_6}$$

NOMENCLATURE

K_h	Polymer hydrolysis rate, day^{-1}
K_{S1}	Saturation constant for acidogens, g L^{-1}
K_{S2}	Saturation constant for syntrophs A, g L^{-1}
K_{S3}	Saturation constant for hydrogenotrophicmethanogens vis-à-vis of H_2, g L^{-1}
K_{S4}	Saturation constant for hydrogenotrophic methanogens vis-à-vis of CO_2, g L^{-1}
K_{S5}	Saturation constant for acetoclastic methanogens, g L^{-1}
K_{S6}	Saturation constant for syntrophs B, g L^{-1}
Kla3	Gas-liquid mass transfer coefficient for H_2, day^{-1}
Kla4	Gas-liquid mass transfer coefficient for CO_2, day^{-1}
Kla7	Gas-liquid mass transfer coefficient for CH_4, day^{-1}
MH_2	Molar mass of H_2, g mol^{-1}
CO_2	Molar mass of CO_2, g mol^{-1}
CH_4	Molar mass of CH_4, g mol^{-1}
P_T	Total pressure (gas phase), atm
Q	Substrate input volumetric flow rate, m^3 day^{-1}
r	Reaction rate, day^{-1}
R	universal gas constant, atm L mol^{-1} K^{-1}
S_i	Concentration of entity i, g L^{-1}
S_i^*	Liquid phase saturation concentration of substance i, g L^{-1}
$S_{i_{in}}$	Input concentration of entity i, g L^{-1}
t	Time, days
T	Temperature, K
V	Liquid phase volume, L
V_g	Gas phase volume, L
X_1	Acidogens concentration, g L^{-1}
X_2	Syntroph A concentration, g L^{-1}
X_3	Hydrogenotrphic methanogen concentration, g L^{-1}
X_4	Acetoclatstic methanogen concentration, g L^{-1}
X_5	Syntroph B concentration, g L^{-1}
$Y_{Si/Sj}$	Yield of S_j from S_i, g g^{-1}
$Y_{Si/Xj}$	Yield of X_j from S_i, g g^{-1}
μ	specific growth rate, day^{-1}
in	Inlet
MAX	Maximum
AcoD	Anaerobic co-Digestion
muMAX1	Maximum acidogens growth rate
muMAX2	Maximum syntrophs A growth rate
muMAX3	Maximum hydrogenotrophic methanogens growth rate
muMAX4	Maximum acetoclastic methanogens growth rate
muMAX5	Maximum syntrophs B growth rate